

FRIGA, a new approach to identify isotopes and hypernuclei in n -body transport models

A. LE FÈVRE⁽¹⁾, Y. LEIFELS⁽¹⁾, J. AICHELIN⁽²⁾, CH. HARTNACK⁽²⁾, V. KIREYEV⁽³⁾
and E. BRATKOVSKAYA⁽⁴⁾⁽¹⁾

⁽¹⁾ *GSI Helmholtzzentrum für Schwerionenforschung - Darmstadt, Germany*

⁽²⁾ *Subatech - Nantes, France*

⁽³⁾ *JINR - Dubna, Russia*

⁽⁴⁾ *FIAS and ITP - Frankfurt-am-Main, Germany*

received 10 January 2017

Summary. — We present a new algorithm to identify fragments in computer simulations of relativistic heavy-ion collisions. It is based on the simulated annealing technique and can be applied to n -body transport models like the Quantum Molecular Dynamics. This new approach is able to predict isotope yields as well as hypernucleus production. In order to illustrate its predicting power, we confront this new method to experimental data, and show the sensitivity on the parameters which govern the cluster formation.

1. – Introduction

In heavy-ion reactions at energies between 20 A MeV and several A GeV, many clusters are formed. This cluster formation presents a big challenge for transport models in which nucleons are the degrees of freedom which are propagated. Identifying clusters in a transport code which transports nucleons is all but simple and therefore in many approaches the fragment formation is simply omitted. This invalidates the prediction of single particle observables as well, because the cluster formation —and therefore the modification of the single particle spectra due to the fragment formation— depends on the phase space region and, as a consequence, cannot be approximated by a momentum-independent scaling factor.

The simplest way to identify clusters is by employing coalescence or a minimum spanning tree procedure. The first needs a multitude of free parameters, whereas the second allows only for an identification at the end of the reaction which excludes any study on the physical origin [1]. In addition, quantum effects, like additional binding energies due to closed shells or pairing energies, are not supplied by the underlying transport theory which is semi-classical.

2. – The principles of the fragment recognition

If one wants to identify fragments early, while the reaction is still going on, one has to use the momentum as well as the coordinate space information. An idea on how to do this has been launched by Dorso and Randrup [2]. It has been further developed into the Simulated Annealing Clusterisation Algorithm (SACA) [3] in the late 1990’s and has been successfully applied to understand the measured fragment charge distribution and spectra as well as bimodality [4,5]. Starting from the positions and momenta of the nucleons at a given time during the reaction, nucleons are combined in all possible ways into fragments or single nucleons applying a simulated annealing technique. Neglecting the interaction among nucleons in different clusters, but taking into account the interaction among the nucleons in the same fragment, this algorithm identifies that combination of fragments and free nucleons which has the *highest binding energy*. If applied after the time when the energetic initial collisions are over, this most bound configuration has been proven to be close—but not exactly identical as we will show later—to the final distribution of fragments identified by the minimum spanning tree method at the end of the reaction [3]. The reason for this is the fact that fragments are not a random collection of nucleons at the end, but an initial-final state correlation. SACA can be applied at any moment during the reaction and allows therefore for a detailed study of the fragment production mechanism.

In SACA, for accounting the interaction between nucleons, only the bulk Skyrme interaction supplemented by a Yukawa potential is used—which is also the potential used for the propagation of the nucleons in the QMD transport model. To obtain more realistic fragment observables and to be able to predict observables for isotopes and hypernuclei, we employ in our new approach a more realistic interaction and add the secondary decay because the fragments, when identified, have a (moderate) excitation energy. This new approach is dubbed FRIGA (Fragment Recognition In General Application).

3. – The new features of FRIGA

In order to predict the absolute multiplicity of the isotope yields, we have added new features to the SACA cluster identification. They include the asymmetry energy, pairing and quantum effects.

For the asymmetry energy, we adopt the parametrisation from IQMD [6], a transport code which we use in the present article for the transport of nucleons. For a proton the single particle energy thus reads:

$$B_{asy} = E_0 \left(\frac{\langle \rho_B \rangle}{\rho_0} \right)^{\gamma-1} \frac{\rho_n - \rho_p}{\rho_B},$$

where $E_0 = 23.3$ MeV, and ρ_n , ρ_p , ρ_B , ρ_0 are the neutron, proton, baryonic and saturation densities, respectively. In the present work, we take $\gamma = 2$ (“stiff” asymmetry potential).

Another significant part of the binding energy of light isotopes are the shell structure and odd-even effects (pairing). In the conditions of high pressure and temperature where FRIGA is used to determine the pre-fragments, these structure effects are not well known. Khan *et al.* [7,8] showed that there are some indications that they affect the primary fragments. The authors demonstrate that the pairing vanishes above a nuclear temperature $T_V \approx 0.5\Delta_{pairing}$ (pairing energy). At normal density the pairing energy

tends to be negligible for heavy nuclei, with $\Delta_{pairing} = \frac{12}{\sqrt{A}}$ MeV, whereas it is strong for light isotopes, like ${}^4\text{He}$ and ${}^3\text{He}$ with 12 MeV and 6.9 MeV, respectively. In FRIGA, the primary fragments are usually produced slightly below the saturation density (typically around half of it) and quite cold, with $T < 1\text{-}2$ MeV, and hence below T_V . Therefore, one cannot neglect the pairing energy. The same is true for shell effects which produce experimentally a visible enhancement of the fragment yield for closed shell nuclei.

In order to determine the contribution of all structure effects to the binding energy of clusters, we make two hypotheses independent of the density and the average kinetic energy of the fragment environment.

First, the relative ratio of this nuclear structure contribution to the overall binding energy remains unchanged at the moderate temperatures and at the density at which clusters are formed which is not far away from the saturation density.

After the nucleus is initialised with the right root-mean-square radius, introducing the two-body interactions between nucleons, which corresponds in infinite matter to the Skyrme equation of state, the total fragment energy

$$(1) \quad E_B(N, Z) = \langle H \rangle = \langle T \rangle + \langle V \rangle \\ = \sum_i \frac{p_i^2}{2m_i} + \sum_i \sum_{j>i} \int f_i(\mathbf{r}, \mathbf{p}, t) V(\mathbf{r}, \mathbf{r}', \mathbf{p}, \mathbf{p}') f_j(\mathbf{r}', \mathbf{p}', t) d\mathbf{r} d\mathbf{r}' d\mathbf{p} d\mathbf{p}',$$

where f_i is the single-particle Wigner density,

$$(2) \quad f_i(\mathbf{r}, \mathbf{p}, t) = \frac{1}{\pi^3 \hbar^3} e^{-\frac{2}{L}(\mathbf{r}-\mathbf{r}_i(t))^2} e^{-\frac{L}{2\hbar^2}(\mathbf{p}-\mathbf{p}_i(t))^2},$$

reproduces very well the nuclear binding energy given by the Weizsäcker mass formula for ground state nuclei, B_0 ([9], fig. 12).

Our second hypothesis is that the extension of the wave packet of eq. (2) remains the right description for the binding energy if the nuclei are deformed or excited when the fragments are identified by the FRIGA algorithm.

Taking both assumptions together, we can express the nuclear structure contribution to the binding energy of a deformed cluster with Z protons and N neutrons in the following way:

$$B_{struct} = E_B(N, Z) \frac{B_{exp}(Z, N) - B_{BW}(Z, N)}{V_{BW}(Z, N) + S_{BW}(Z, N)}$$

where B_{exp} is the experimentally measured binding energy, and B_{BW} , V_{BW} and S_{BW} are, respectively, the binding energy without pairing, the volume and surface terms of the Bethe-Weizsäcker formula. (Hyper-)Isotopes which are known not to be bound in their ground state, are discarded in FRIGA by assigning to them a very repulsive B_{struct} . The total binding energy of a cluster with N and Z , which is used in the annealing algorithm, will then be

$$B = E_B(N, Z) + B_{asy} + B_{struct}$$

in contradistinction to SACA in which only the first term is used.

Figure 1 shows the influence of the asymmetry energy and of the structure energy on the isotope yield in the reaction ${}^{124}\text{Xe} + {}^{112}\text{Sn}$ at 100 A MeV. We display here the

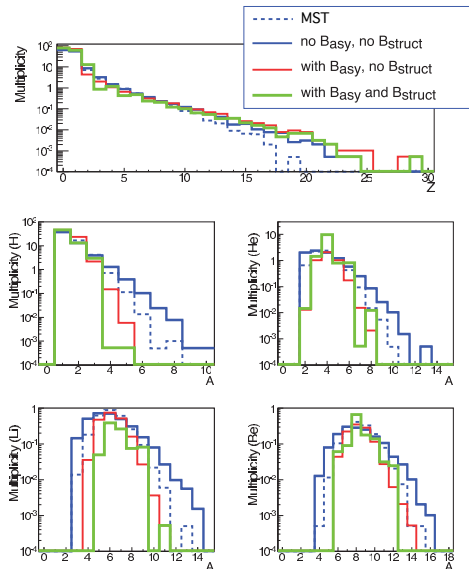


Fig. 1. – IQMD predictions for the central ($b < 0.2b_{max}$) collisions of $^{124}\text{Xe} + ^{112}\text{Sn}$ at 100 A MeV incident energy. Dashed line for the MST (coalescence) algorithm alone (performed at the late time 200 fm/c), blue line for the initial SACA model, which has been extended into FRIGA with an asymmetry term (red) and additional nuclear structure contribution (green). The top panel shows the mean multiplicity distribution of fragments as a function of their charge. The four others depict the yields of H, He, Be and Li isotopes.

results for central collisions ($b < 0.2 b_{max}$). This figure illustrates as well how the various ingredients influence the fragment yield obtained in FRIGA, assuming an early clusterisation at $t = 60$ fm/c. From that time on, the size of the pre-fragments does not change anymore, unlike MST which needs a longer time to stabilise the fragment partitions (here 200 fm/c). It corresponds to the passing time of the colliding system which we found as the general rule —independent of its size and incident energy. We see that the charge distributions are not strongly modified for the different options, whereas details of the isotopic yield are strongly influenced: the asymmetry energy tends to narrow the distributions towards the valley of stability, whereas the structure effects contribute to restore the natural abundances, particularly strong for the ^4He clusters.

4. – Excitation energy and density of the primary fragments

The pre-fragments, called also “primary” fragments, created in FRIGA, are often produced non-relaxed in shape and density. When turning to their ground state, the shape surface energy is converted into excitation energy. Using QMD simulations, for beam energies between 50 A MeV and 1 A GeV, FRIGA obtains for central heavy ion collisions a mean excitation energy of the intermediate mass fragments between 0 and 3 A MeV, depending on the fragment size and very similarly to the experimental measurements of [10]. This excitation energy is sufficiently large that the secondary decay of the pre-fragments causes a significant contribution to the yield of small clusters. For this reason, we optionally allow in FRIGA the excited cluster to undergo sequential secondary decays, using the GEMINI algorithm [11].

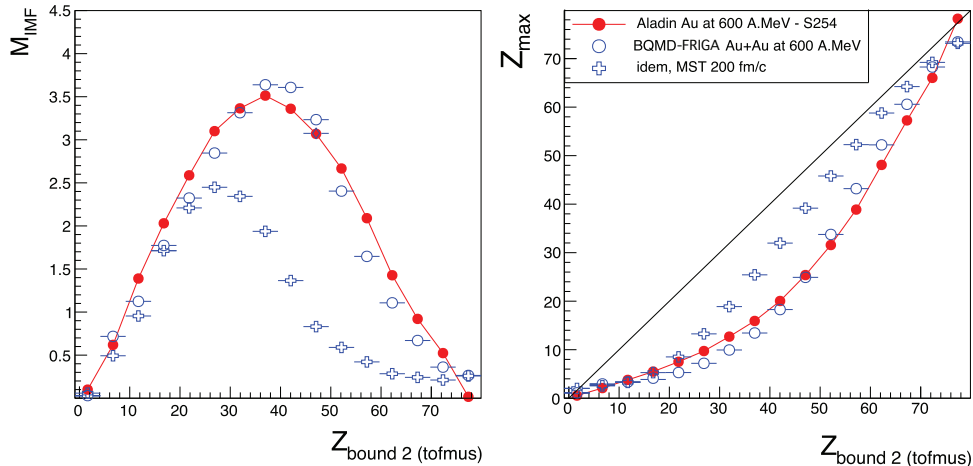


Fig. 2. – Predictions of FRIGA from BQMD [9] simulations of Au+Au at 600 A MeV incident energy (open circles) compared with ALADiN experimental data (full symbols, results of the S254 experiment combining the TOF and MUSIC data, courtesy of the ALADiN Collaboration). Observables concern the projectile spectator. Left and right panels show, respectively, the mean multiplicity in an event of intermediate-mass fragments with $Z > 2$, and the mean highest-fragment charge, as a function of the total charge of fragments with $Z > 1$ (Z_{bound2}) which scales with the centrality of the collision [12]. The result of the coalescence (MST) is depicted by open crosses.

Another interesting feature of the primary clusters in FRIGA is their internal density. Although the medium is close to ρ_0 , at the stage of the collision when the primary cluster formation is stabilised, just after the colliding system begins to separate, the fragments predicted by FRIGA are produced quite dilute, typically around $\rho = \rho_0/2$ for intermediate mass fragments, and around $\rho = \rho_0/5$ for the light $Z < 3$ isotopes. This is explained by the fact that the dense clusters are disfavoured, because they would contain nucleons which are moving against each other. In this case the nucleons have a too high relative momenta to form a cluster. Therefore, in the FRIGA approach, fragment formation tests only the low density behaviour of the potentials, which are contributing to the binding energy.

5. – Achievements of FRIGA in the multifragmentation regime

We have seen in *e.g.* [4, 5] that the FRIGA approach is successful in predicting the fragment charge distributions and spectra as well as bimodality measured in heavy-ion collisions in the intermediate energy regime. At relativistic energies, the same prediction power is observed in the spectator fragmentation, as illustrated by fig. 2, being able to reproduce the well-known “rise and fall” phenomenon (top panel) published in [12], as well as the centrality dependence —here given by Z_{bound2} — of the highest fragment charge. In this figure, we see again that a simple coalescence approach fails. However, we have observed that the FRIGA approach still strongly underestimates the light isotope yields created in the mid-rapidity (fireball) region, as measured, *e.g.*, in [13]. The reason is that at relativistic energies the temperature and the entropy generated in the fireball are so high that the pre-fragments are mostly unbound at early times. They need a

relatively longer time to reach a bound configuration than in the central collisions at intermediate energies. Therefore, in this situation, determining the fragments at a single time—as done in FRIGA up to now—is not suited. A new strategy to circumvent this limitation in FRIGA is presently under development.

6. – Another application of FRIGA: the hypernucleus formation

A hypernucleus is a nucleus which contains at least one hyperon ($\Lambda(uds), \dots$) in addition to nucleons. Extending FRIGA to the strange sector requires the knowledge of the ΛN potential. In this first study, we consider the strange quark as inert and use $V_{\Lambda N} = \frac{2}{3}V_{nN}$ for protons as well as for neutrons. Similarly, we consider the case of multiple strange nuclei as well, in which more than one hyperon is part of the fragment. There, the coupling of 2 Λ 's contributes with the potential $V_{\Lambda\Lambda} = (\frac{2}{3})^2V_{nN}$. In the present approach we neglect B_{asy} for the hyperons, and take the contribution of the core nucleus (partner of the hyperons) as if it were decoupled from the hyperon. Since the pairing and shell contributions in the binding energy are not yet well known for hypernuclei, we neglect the B_{struct} contribution.

Using these modifications of the potentials, FRIGA produces hypernuclei with the same procedures as non strange fragments. In the underlying QMD-like programs, which propagate the hadrons, Λ 's are produced in different reactions: $\bar{K} + N \rightarrow \Lambda + \pi$, $\pi + n \rightarrow \Lambda + K^+$, $\pi^- + p \rightarrow \Lambda + K_0$, $p + p \rightarrow \Lambda + X$. Their abundance, position and momentum distributions are strongly influenced by the reaction kinematics, the nuclear equation of state and the in-medium properties of the K^+ (kaon potential, etc.) which are implemented in the transport model [14].

Due to their composition, the yields of hypernuclei are produced when a cluster in coordinate and momentum space absorbs a hyperon. In heavy-ions collisions at relativistic energies, the hyperon distributions are strongly peaked around the mid-rapidity region whereas the large fragments have rapidities close to the beam or target rapidity. The closer the rapidity of the hyperon approaches—by production or by subsequent collisions—the target/beam rapidity, the larger is the probability that it can be absorbed by one of the larger clusters. Heavy hypernuclei are therefore observed not far away from beam/target rapidity. At the same time hyperons can also form with other nucleons light clusters at mid-rapidity. There, the probability decreases with the cluster size because it is increasingly difficult to form large cluster out of a gas of nucleons. Whereas the large clusters in the beam/target rapidity regime can be identified quite early, the light clusters at mid-rapidity are formed later and many of them decay due to the interactions with the surrounding nucleons which form a gas of a large temperature as compared to the cluster binding energy. This is illustrated in fig. 3.

As seen previously, in fig. 1, the ingredients of the cluster binding energy influence the light isotope yields in FRIGA. The same is observed for hypernuclei. Adopting the factor $\frac{2}{3}$ in $V_{\Lambda N}$ has a strong effect, decreasing on the average the hypernucleus yields by around 20 percent. The asymmetry energy in the cluster can have a similar effect, depending on the isotope (Z, N) asymmetry.

In order to illustrate the predicting power of the FRIGA algorithm, we confront it to experimental observations of light hypernuclei produced in the spectator region in collisions of the light system ${}^6\text{Li} + {}^{12}\text{C}$ at 2 AGeV incident energy, measured by the HyPHI Collaboration at the SIS synchrotron of GSI Darmstadt. The data presented here are taken from [15]. Figure 4 compares the IQMD-FRIGA predictions for the rapidity distributions of ${}^3_{\Lambda}\text{H}$ and ${}^4_{\Lambda}\text{H}$ with the experiment. The best agreement in the experimentally

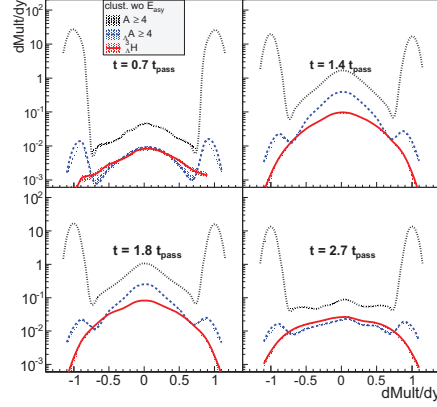


Fig. 3. – Predictions of FRIGA from PHSD [16] simulations of Au+Au collisions at 11.45 A GeV incident energy, $b = 6$ fm, showing the multiplicity per event as a function of the rapidity in the centre of the collision scaled to the projectile rapidity, for various (hyper-)clusters (A_{Λ} are hyper-clusters with $A \geq 4$) and clusterisation times. $t_{pass} = 7.5$ fm/c is the passing time of the projectile and target in central collisions. Like in fig. 4, the shaded areas depict the statistical uncertainties.

resolved rapidity region (close to the projectile spectator, $y/y_{beam} > 0.7$) has been obtained while excluding the most central collisions (taking $b > 3$ fm). This procedure is a very basic approach to the simulate the effect of the complex experimental trigger. The chosen rapidity region has the highest hadronic yield and contains still the tail of the Λ distribution, as predicted by IQMD-FRIGA. At these rapidities, the experiment has measured a yield ratio $Y({}_{\Lambda}^3\text{H})/Y({}_{\Lambda}^4\text{H}) = 1.4 \pm 0.8$, with which IQMD-FRIGA agrees

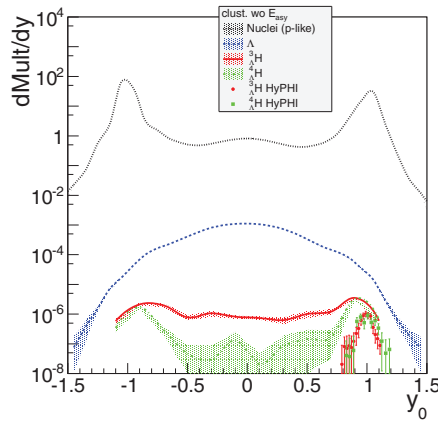


Fig. 4. – Predictions of FRIGA (clustering at $2t_{pass}$, binding energy excluding B_{asy}) from IQMD simulations of ${}^6\text{Li} + {}^{12}\text{C}$ collisions at 2 A GeV incident energy, $b > 3$ fm compared to the HyPHI experimental data. The results of the model calculations are not filtered for the experimental acceptance. It shows the multiplicity per event per unit of rapidity, as a function of the rapidity in the centre of the collision scaled to the projectile rapidity, for all clusters (in proton-like weighting), Λ 's, ${}_{\Lambda}^3\text{H}$ and ${}_{\Lambda}^4\text{H}$. Markers are experimental data.

within the experimental uncertainty with 1.3 ± 0.2 . Including the asymmetry contribution B_{asy} in the cluster binding energy in FRIGA, we obtain a yield ratio of 1.9 ± 0.4 which is still within this uncertainty. Therefore, at this level, the role of the asymmetry energy is difficult to judge.

7. – Conclusion

We present here the first step towards an understanding of the production of isotopic yields and hypernuclei in heavy ion reactions. Our clusterisation algorithm FRIGA, an improved version of the SACA approach, which includes pairing and asymmetry energies as well as other structure effects is able to describe more precisely the nuclear binding energy and allows for realistic predictions of absolute (hyper-)isotope yields. We have seen that the asymmetry and pairing potentials can have a strong influence on both, the yields and momentum anisotropies for the (hyper-)isotopes. According to this model, the nucleons which form fragments have initially a fairly low density. They contract and form finally slightly excited fragments which may undergo secondary decays. Therefore, the fragment formation is sensitive to the density dependence of the asymmetry energy and the pairing energy. However, fragments test this dependence only for densities below the saturation density.

REFERENCES

- [1] GOSSIAUX P. B., PURI R. K., HARTNACK CH. and AICHELIN J., *Nucl. Phys. A*, **619** (1997) 379.
- [2] DORSO C. O. and RANDRUP J., *Phys. Lett. B*, **301** (1993) 328.
- [3] PURI R. K. and AICHELIN J., *J. Comput. Phys.*, **162** (2000) 245; VERMANI Y. K. and PURI R. K., *EPL*, **85** (2009) 62001.
- [4] ZBIRI K., LE FÈVRE A., AICHELIN J. *et al.*, *Phys. Rev. C*, **75** (2007) 034612.
- [5] LE FÈVRE A. *et al.*, *Phys. Rev. C*, **80** (2009) 044615.
- [6] HARTNACK CH. *et al.*, *Eur. Phys. J. A*, **1** (1998) 151.
- [7] KHAN E., NGUYEN VAN GIAI and SANDULESCU N., *Nucl. Phys. A*, **789** (2007) 94.
- [8] KHAN E., GRASSO M. and MARGUERON J., *Phys. Rev. C*, **80** (2009) 044328.
- [9] AICHELIN J., *Phys. Rep.*, **202** (1991) 233.
- [10] INDRA COLLABORATION (HUDAN S. *et al.*), *Phys. Rev. C*, **67** (2003) 064613.
- [11] CHARITY R. J. *et al.*, *Nucl. Phys. A*, **476** (1988) 516.
- [12] SCHÜTTAUF A. *et al.*, *Nucl. Phys. A*, **607** (1996) 457.
- [13] REISDORF W. *et al.*, *Nucl. Phys. A*, **848** (2010) 366.
- [14] HARTNACK CH., OESCHLER H., LEIFELS Y., BRATKOVSKAYA E. L. and AICHELIN J., *Phys. Rep.*, **510** (2012) 119, arXiv:1106.2083 [nucl-th].
- [15] RAPPOLD CH. *et al.*, *Phys. Lett. B*, **747** (2015) 129.
- [16] CASSING W. and BRATKOVSKAYA E. L., *Nucl. Phys. A*, **831** (2009) 2.